J Mater Sci (2007) 42:7446–7450
DOI 10.1007/s10853-007-1605-y

Physical origin of spontaneous interfacial alloying in immiscible W/Cu multilayers

Pascale Villain · Philippe Goudeau · Frederic Badawi · G. Ouyang · G. W. Yang · Véronique Pélosin

Received: 30 June 2006 / Accepted: 12 February 2007 / Published online: 18 May 2007
© Springer Science+Business Media, LLC 2007

Abstract A metastable solid solution has been observed in immiscible W/Cu multilayers sputter deposited with very low period (≤ 3 nm). A recent model evidencing size dependence of surface energies and diffusion coefficients in bilayers may explain the observed trends since diffusion coefficients highly increase when layer thickness decreases. Furthermore, implantation effects of the energetic incoming atoms during layer deposition undoubtedly reinforce these mixing phenomena.

Introduction

Refractory metals such as tungsten were used as diffusion barrier between copper conductors and silicon substrates in microelectronic circuits since these two metals are considered as immiscible and thus do not alloy in the bulk. Based on the equilibrium thermodynamics, the interfaces in binary immiscible metallic systems such as W/Cu bilayers should be sharp. However, it has been reported that substitution surface alloying may occur when Cu is deposited on a W (001) surface [1, 2]. This alloying possibility depends on atomic sizes, nature of atomic bondings, and coordination numbers. Experimental studies have also shown that ion beam mixing of W/Cu multilayers as well as co-sputtering of Cu and W can lead to metastable W–Cu alloys and compounds [3, 4], which has been confirmed by ab initio calculations [5]. In a recent paper, Ouyang et al. [6] developed a model for the diffusion at the interface between two layers evidencing an anomalous interfacial diffusion in immiscible metallic bilayers related to size-dependent diffusion coefficients. The Cu/Ta system was given as an example. This letter deals with the W/Cu system; experimental results indicate that copper may be found in the tungsten sublayers of W/Cu multilayers when the period is reduced down to 3 nm [7], and they are consistent with the results of the size-dependent diffusion model.

P. Villain (✉) · P. Goudeau · F. Badawi
Laboratoire de Métallurgie Physique UMR 6630 CNRS/Université de Poitiers, SP2MI, BP 30179, 86962 Futuroscope Chasseneuil cedex, France
e-mail: pascale.villain@univ-poitiers.fr

G. Ouyang · G. W. Yang
Sate Key Laboratory of Optoelectronic Materials and Technologies, School of Physics Science and Engueering, Zhongshan University, Guangzhou 510275, P.R. China

V. Pélosin
Laboratoire de Mécanique et Physique des Matériaux UMR 6617 CNRS/ENSMA, BP 40109, 86961 Futuroscope Chasseneuil cedex, France

Experimental set up

W/Cu multilayers were deposited onto 650 µm thick naturally oxidised (100) silicon wafers by ion beam sputtering at room temperature in a Nordiko-3000 device, tungsten being the first deposited layer. It should be noted that although the substrate holder is water-cooled, the temperature might increase by about 40 °C during the deposition process. The total thin film thickness ranges between 220 nm and 260 nm.

Several characterisation experiments have been done. X-ray reflectivity measurements were performed to deduce the modulation wavelength Λ (thickness of one W/Cu bilayer) from the small angle Bragg's peak positions.

Table 1 Main parameters characterizing the studied specimens: multilayer period Λ, number of W/Cu pairs, atomic composition, mean thickness of each individual layer (e_W and e_{Cu}), and stress-free lattice parameter of tungsten (a_0)

Λ (nm)	Number of pairs	At% W	e_W (nm)	e_{Cu} (nm)	a_0 (W) (nm)
3.1 ± 0.1	70	56 ± 1%	2.0 ± 0.1	1.1 ± 0.1	0.314
5.7 ± 0.1	35	56.5 ± 1%	3.6 ± 0.1	2.1 ± 0.1	0.316
24.0 ± 0.1	10	48 ± 1%	13.3 ± 0.1	10.7 ± 0.1	0.318
2.6 ± 0.1	100	53 ± 1%	1.6 ± 0.1	1.0 ± 0.1	0.313

Atomic proportions of tungsten and copper were determined thanks to Electron Dispersive X-ray Spectroscopy (EDXS) measurements. The mean thickness of tungsten (e_W) and copper (e_{Cu}) individual sublayers was deduced from Λ and the atomic proportions, assuming the density of each material is equal to the bulk one. Large angle X-ray diffraction (XRD) measurements were realised in asymmetric configuration to determine the stress-free lattice parameters of tungsten layers by means of the ''$\sin^2\psi$ method''; in fact, this technique allows decoupling the effects of stresses and of the microstructure on the measured lattice parameters [8]. Bulk tungsten elastic constants were used for this determination. All parameters of the specimens are reported in Table 1. Conversion electron Extended X-ray Absorption Fine Structure (EXAFS) measurements were performed at the French synchrotron radiation facility L.U.R.E. (Orsay, France) on the D42 beam line on the Cu-K and W-L_{III} absorption edges so as to investigate the local order around W and Cu atoms. In situ annealing experiments were also realised on the Λ = 3 nm specimen in a Brucker D8 X-ray diffractometer. The temperature was increased from 20 °C to 660 °C by increments of 10 °C with a temperature rate of 5 °C/min; diffractograms were recorded during 180 s at each temperature step thanks to a position sensitive detector (PSD).

X-ray results and discussion

X-ray diffraction measurements showed that the stress-free lattice parameters (a_0) of the tungsten sublayers is smaller than the bulk one (a_{bulk} = 0.3165 nm) in the small period multilayer, whereas it is larger in the other specimen [9]. This observation reveals important differences in the microstructure of these two specimens. It may be accounted for by a vacancy-type structure and columnar grain morphology with nanometer-sized intergranular voids when the sublayers are the thinner, a densified structure with interstitial incorporation when the sublayer thickness increases. Another interpretation may be that some copper atoms substitute for tungsten ones in tungsten lattice resulting in a decrease of the lattice parameter and thus to a shift of the diffraction peaks towards higher 2θ angles. To verify this assumption, EXAFS measurements have been carried out. Simulations of the spectra show the presence of Cu atoms in the W layers (up to 12 at% for the lower period, Λ = 3 nm) [7].

This experimental evidence of copper mixing in tungsten layers has been confirmed by complementary experiments. Firstly, tungsten thickness has been reduced while keeping constant copper thickness; the main parameters of this specimen are given at the bottom of Table 1. XRD measurements have been performed using a two-circle goniometer, a copper rotating anode and a position sensitive detector. Due to the W <110> texture, the pole direction $\psi \sim 30°$ has been chosen for the measurement; it is achieved with the Ω configuration setting the incident angle at ~6.5°. Results are shown on Fig. 1; the shift of the (211)-W diffraction peak towards larger 2θ angles (corresponding to smaller interatomic distances) is clearly visible for the Λ = 3 nm specimen and is stronger for the smallest period specimen. In a second step, a series of multilayers has been prepared with constant tungsten thickness (1.5 nm) and variable average copper thickness ranging from 0 up to 1 nm [10]. Unfortunately, there are major difficulties in comparing XRD measurements for the extreme value of copper thickness, related to strong texture variations. For very low copper thickness, discontinuous Cu layers lead to two tungsten texture components (<110> and <111>), copper contribution being rather small; on the contrary when copper thickness is larger, only one tungsten texture component is observed (<110>) with a very low intensity compared to the very strong Cu<111> contribution. It is then not possible to conclude on this series of samples.

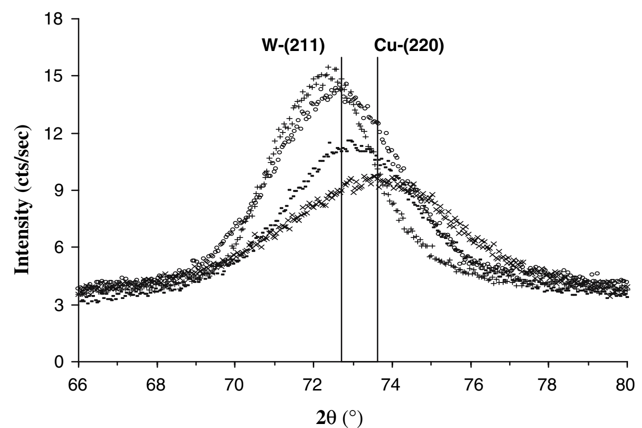

Fig. 1 Evolution of the W-(211) diffraction peak as a function of the period thickness: (+) 24 nm, (o) 6 nm, (-) 3 nm and (x) 2.5 nm (Ref. 7)

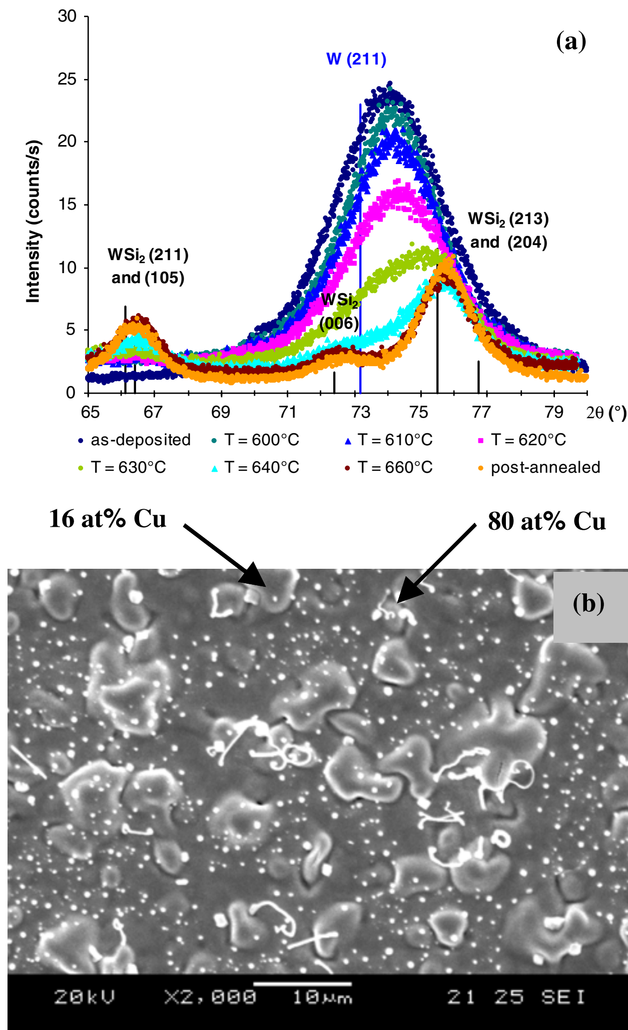

Fig. 2 (**a**) X-ray diffraction diagrams recorded during the in situ annealing experiment on the $\Lambda = 3$ nm specimen; they correspond to the angular domain where the α-W(211) diffraction peak appears. (**b**) SEM image (with secondary electrons) of the surface of the annealed sample; copper nodules appears as white points on a grey background formed of tungsten silicide WSi_2. The atomic percentages of Cu were determined by an EDXS analysis (beam energy = 20 keV, probe-size ≈ 1 µm^2). Film buckling structures due to the thermal stresses and volume increase during phase transformation are clearly visible

Since, W and Cu are immiscible in the bulk state, solid solution demixing may be achieved upon annealing. As it can be seen on Fig. 2a, no evolution of the W diffraction peak appears until Si diffuses at 600 °C from the substrate through the tungsten layers and forms a WSi_2 phase. Scanning Electron Microscopy (SEM) observations in a JEOL 5600 V microscope with backscattered and secondary electrons have shown that a silicide layer has grown on the whole Si surface while small Cu nodules has formed from pure copper layers, with diameter less than 1 µm (Fig. 2b). Since, no demixing of W(Cu) layers has been observed for temperatures up to 600 °C, this solid solution seems to be very stable in this low period multilayer; it is probably stabilised by the interfaces. Similar phenomena have been observed in the case of a Ta barrier layer between a Si substrate and a Cu layer [11].

Modelling and discussions

These experimental results can be interpreted in both thermodynamics and kinetics. In thermodynamic, the size-dependent solid–solid interface energy in binary multilayers is described as follows, [12]

$$\gamma_{ss}^{WCu}(D) = \gamma_{sso}^{WW}[1 - h_W/(2D)] + \gamma_{sso}^{CuCu}[1 - h_{Cu}/(2D)] \quad (1)$$

where $\gamma_{ss}^{WCu}(D)$, γ_{sso}^{ii} (ii = WW,CuCu), h_i (i = W,Cu) and D are the size-dependent solid–solid interfacial free energy, the corresponding bulk value, the diameter of atoms in tungsten and copper and the thickness of bilayers, respectively. Note that γ_{sso} can be determined by Gibbs–Thomson's equation. We define the factor of ΔF to be the interface alloying driving force. Thus, for binary immiscible W/Cu multilayers, ΔF can be expressed as: [12]

$$\Delta F = S_f \gamma_{ss}^{WCu}(D) - \Delta H \quad (2)$$

where S_f is the surface area occupied by one mole of interfacial atoms. ΔH is the heat of formation of the alloy. For copper/tungsten system, ΔH is +33 kJ mol^{-1} [12]. S_f is therefore expressed as $S_f = \alpha_W S_{fW} + \alpha_{Cu} S_{Cu}$, in which α_W and α_{Cu} are the fractions of interfacial atoms W and Cu versus the total atoms in multilayers. Here, $\alpha_W = x_W h_W/L_W$ and $\alpha_{Cu} = x_{Cu} h_{Cu}/L_{Cu}$ where L_W and L_{Cu} are the thickness of original interface layer shown in Fig. 3 and x is the atomic concentration. Note that the thickness of interface is assumed an atomic layer. The interfacial alloying phase diagram in Fig. 4 can be obtained by Eq. 2. The curve separating the alloying (M) and non-alloying (N) domains is defined by $\Delta F = 0$. Evidently, there is alloying when $\Delta F > 0$. Interestingly, we can see the theoretical

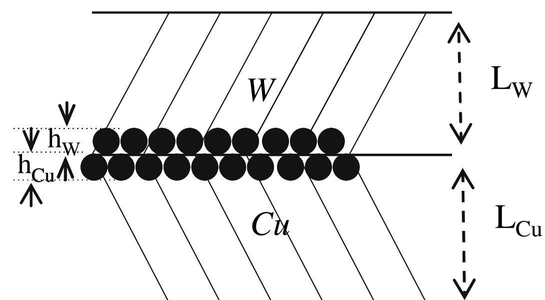

Fig. 3 Schematic illustration of binary immiscible metallic bilayered films with components W and Cu; h refers to the diameter of atoms and L is the layer thickness

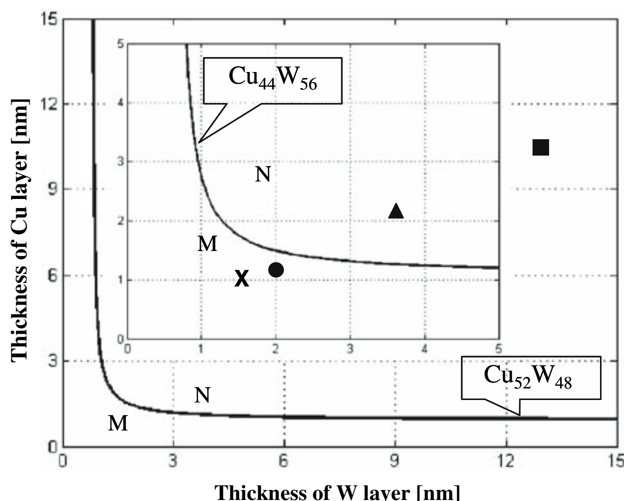

Fig. 4 Interface alloying phase diagram in copper/tungsten bilayers. The inside is $Cu_{44}W_{56}$ while the outer is $Cu_{52}W_{48}$. The two letters M and N denote alloying phase and non-alloying phase and symbols (×), (●), (▲), (■) are corresponding experimental results

predictions are in good agreement with the experimental results.

In kinetics, anomalous interdiffusion will occur at the interface. Based on the recent letter, the size-dependent diffusion coefficients and diffusion time can be calculated [6]. These results are shown in Fig. 5. Clearly, we can see that copper diffusion into tungsten is more rapid than tungsten diffusion into copper. Also, the diffusion coefficient for Cu diffusing in W is higher than the one for W diffusing in Cu in Fig. 5a. These diffusion coefficients are size-dependent: they strongly increase when the layer thickness is reduced below 2 nm. In Fig. 5b, the diffusion time with tungsten in copper is much longer than copper in tungsten. Therefore, the copper/tungsten solid solution can be formed at temperature 340 K during the deposition time in the case of Λ = 3 nm multilayers. The above corresponding calculating parameters are listed as h_{Cu} = 0.2556 nm, h_W = 0.2741 nm [15], $S_f^{Cu} = 1.67 \times 10^5$ m^2 mol^{-1}, $S_f^{W} = 2.03 \times 10^5$ m^2 mol^{-1} [16].

Then it clearly appears that the thermodynamic and kinetic models give trends in agreement with experimental facts: W and Cu become to a certain extent miscible when the layer thickness is reduced below 2 nm due to the sharp increase of the diffusion coefficients. The diffusion of Cu into W is easier than the diffusion of W into Cu. However, in the model, a static situation is involved whereas in the experiment, the incoming atoms during the deposition process posses a kinetic energy ranging from 10 eV to 100 eV. Implantation depths $R_p + \Delta R_p$ calculated by means of the TRIM Code [17] are 0.4 nm and 0.9 nm, respectively; R_p is the projected range and ΔR_p the longitudinal straggling. These penetration depths are not negligible considering sublayer thicknesses in the case of the

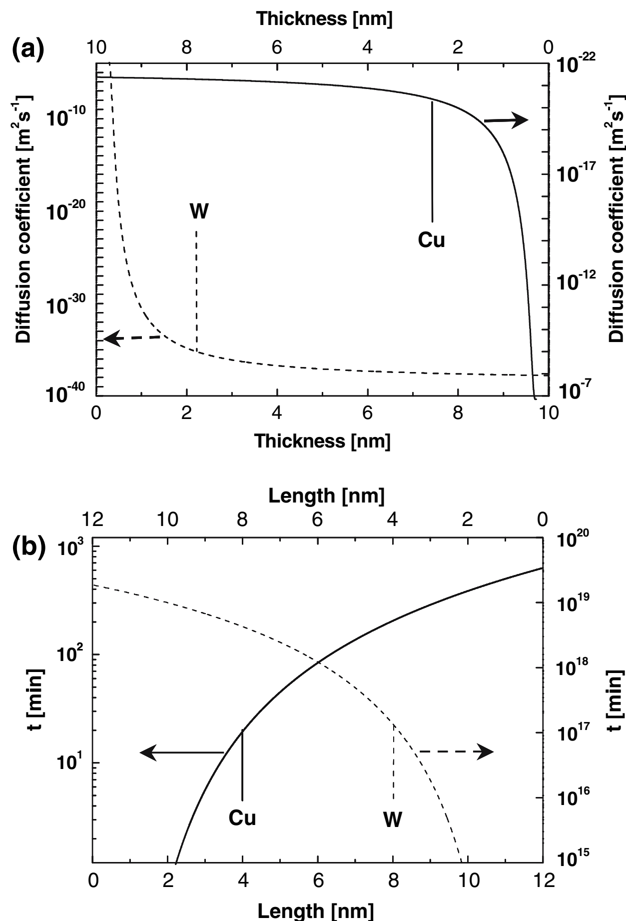

Fig. 5 Size-dependent diffusion coefficients (**a**) and diffusion time (**b**) in copper/tungsten bilayer system at temperature 340 K. In calculations, these parameters are used as follows, $D_0^{W \to Cu} = 1.69 \times 10^{-4}$ m^2 s^{-1}, and E_∞ = 225.7 kJ mol^{-1} (Ref. 13). $D_0^{Cu \to W} = 1.4 \times 10^{-7}$ m^2 s^{-1}, and E_∞ = 96.6 kJ mol^{-1} (Ref. 14)

Λ = 3 nm and Λ = 2.5 nm multilayers (Table 1); thus this implantation effect may also be one of the main factors leading to the formation of the solid solution. This assumption is reinforced by the slight mixing effect observed via EXAFS measurements in the Λ = 6 nm multilayer, in contradiction with calculation predictions (Fig. 4). The model should also be improved concerning the two main following points: it deals with two layers (one layer Cu and one layer W, one interface), not with a multilayer; it considers single crystal layers, not taking into account grain boundary diffusion while in our experimental case, the multilayers are polycrystalline with a columnar microstructure. Work is in progress to model such systems.

Concluding remarks

To summarise, a non-equilibrium solid solution has been observed in the immiscible W–Cu system in the case of

sputter deposited W/Cu multilayers with very low period (≤ 3 nm). Recent thermodynamic and kinetic models evidencing size dependence of surface energies and diffusion coefficients in bilayers may explain the trends observed in multilayers since diffusion coefficients highly increase when layer thickness decrease. Implantation effects of the energetic incoming atoms during layer deposition and grain boundary diffusion in the polycrystalline layers undoubtedly reinforce these mixing phenomena in the case of very small periods. Otherwise, the impact of interface stress is certainly weak since the X-ray stress in tungsten layers and the total stress determined form substrate curvature are similar for the lowest period thicknesses [9].

Acknowledgements The French authors would like to thank M. Piellard for SEM observations and T. Girardeau for EXAFS experiments and analysis. G. Ouyang and G.W. Yang would like to thank the National Science Foundation of the People's Republic of China (90306006) and Natural Science Foundation of Guangdong province (01009737) for support of this work.

References

1. Shu XK, Jiang P, Che JG (2003) Surf Sci 545:199
2. Hu P, Wander A, Morales de la Garza L, Bessent MP, King DA (1993) Surf Sci Lett 286:L542
3. Nastasi M, Saris FW, Hung LS, Mayer JW (1985) J Appl Phys 58:3052
4. Dirks AG, van den Broek JJ (1985) J Vac Sci Technol A 3:2618
5. Zhang RF, Kong LT, Gong HR, Liu BX (2004) J Phys Condens Mat 16:5251
6. Ouyang G, Wang CX, Yang GW (2005) Appl Phys Lett 86:171914
7. Goudeau P, Villain P, Girardeau T, Renault P-O, Badawi KF (2004) Scripta Mat 50:723
8. Noyan IC, Cohen JB (1987) Residual stress measurement by diffraction and interpretation. Springer, New York
9. Villain P, Goudeau P, Renault P-O, Badawi KF (2002) Appl Phys Lett 81:4365
10. Girault B, Villain P, Le Bourhis E, Goudeau P, Renault P-O (2006) Surf Coat Tech 201:4372
11. Laurila T, Zeng K, Kivilahti JK, Molarius J, Suni I (2000) J Appl Phys 88:3377
12. Ouyang G, Wang CX, Li SW, Zhu X, Yang GW (2006) Appl Surface Sci 252:3993
13. Brandes EA, Brooks GB (1992) Smithells metals reference book, 7th edn. Butterworth-Heinemann
14. Melmed AJ (1965) J Chem Phys 43:3057
15. http://www.webelements.com/
16. Chen YG, Liu BX (1997) J Phys D: Appl Phys 30:1729
17. Ziegler JF, Biersack JP SRIM version 2003.20 ''The stopping and range of ions in matter''